Core and Valence-Band Photoelectron Spectroscopic Studies of Nickel Interaction with Etidronic Acid

Yuanling Liang,† Dilip K. Paul,‡ and Peter M. A. Sherwood*,†

Department of Chemistry, Willard Hall, Kansas State University, Manhattan, Kansas 66506, and Department of Chemistry, St. Mary College, Leavenworth, Kansas 66048

Received March 22, 1993. Revised Manuscript Received August 10, 1993®

The corrosion behavior of nickel metal in both sodium chloride and etidronic acid (EDA) solutions was studied by X-ray photoelectron spectroscopy (XPS) and infrared spectroscopy. A polymer film was found to form on the surface of the unoxidized metal after treatment with 1 M EDA. This polymer film can effectively prevent the corrosion of nickel by chloride ions. Sodium chloride solution appears to increase the thickness of the polymer film, and no phosphorous was detected in the film. This indicates that the film was formed by decomposing EDA, rather then by simple adsorption of EDA on the nickel surface. The film was so thick that no nickel XPS signal from the metal and/or its oxides could be seen. The XPS and infrared results were consistent with an oxidized hydrocarbon film containing ether and hydroxide groups. Nickel oxide or oxidized nickel metal exposed to EDA led to the formation of nickel etidronate rather than the polymer film.

Introduction

1-Hydroxyethylidene-1,1-diphosphonic acid (hydroxyethyl diphosphonate or HEDP), or etidronic acid (EDA) and its salts have found widespread use as corrosion inhibitors. These compounds have been used as nonpolluting corrosion inhibitors in paints, in various corrosion protection applications, and as complexing agents.[1-4] EDA and related compounds have been widely investigated as corrosion inhibitors for iron and steel.[5-9] No work has yet been reported as to the behavior of these compounds with nickel metal surfaces.

Corrosion inhibitors can act in various way to inhibit corrosion. Many organic compounds have been used as inhibitors, where it is believed that the inhibitor effect is mainly caused by adsorbing the organic compounds on the metal surface.[3] This adsorbed layer hinders the escape of metal ions from the surface either by blocking the surface or by imposing an electrical field that will oppose the movement of cations away from the surface. Adsorption of inhibitors also decreases the number of sites where aggressive ions can be adsorbed. HEDP (EDA) can act by forming a surface complex that is both lightly colored and provides some corrosion inhibition (e.g., on iron or steel). However in this work we find rather different behavior.

In presenting a study involving the relatively less corrodible nickel metal, one notes that both nickel metal and oxides have been widely used to catalyze the dissociation of organic compounds.[10,11] We show in this paper that clean nickel metal does indeed cause the decomposition of EDA on nickel to give a surface film.

The surface chemistry of the films formed in this work have been examined by X-ray photoelectron spectroscopy (XPS or ESCA) in the core and valence band region. Reflection absorption infrared spectroscopy (RAIR) is a useful tool for the investigation of thin organic films on metal substrates,[12-15] and we have used this method to complement the surface chemical information provided by the XPS studies. The use of the Fourier transform spectrometer has made the acquisition of relatively high resolution spectra (2–4 cm^{-1}) for extremely thin films (< 50 Å) or even a monolayer[14-16] of complex molecules[14] a reality.

In this paper, we report the use of XPS and RAIR for nickel exposed to etidronate solutions in a special anaerobic cell that allows the study of the liquid/solid interface without air exposure. The effectiveness of the resulting surface film against corrosion was monitored by exposure of the resulting surface to sodium chloride solution. The film-forming process was examined by exposing clean and oxidized nickel surfaces to EDA.

Experimental Section

Instrumentation. XPS spectra were collected on a VSW HA100 spectrometer with a second UHV system used for liquid exposure experiments. The design of this chamber and its liquid

† Kansas State University.
‡ St. Mary College.
® Abstract published in *Advance ACS Abstracts,* October 1, 1993.

(1) Good, R. B.; Arots, J. B. *Proc.—Int. Water Conf., Eng. Soc. West. Pa.* **1981**, *42*, 65.
(2) Pallos, G.; Lee, K. H.; Johnson, D. A.; Buss, E. *Mater. Perform.* **1986**, *5*, 32.
(3) Pallos, G.; Wallwork, G. *Corros. Rev.* **1985**, *6*, 237.
(4) Fang, J. L.; Wu, N. J. *J. Electrochem. Soc.* **1989**, *136*, 3800.
(5) Sekine, I.; Hirakawa, Y. *Corrosion* **1986**, *42*, 272.
(6) Airey, K.; Armstrong, R. D.; Handyside, T. *Corrosion Sci.* **1988**, *28*, 449.
(7) Armstrong, R. D.; Airey, K.; Su, F. *Electrochem. Acta* **1989**, *34*, 707.
(8) Walsh, I. D.; Sherwood, P. M. A. *Chem. Mater.* **1992**, *4*, 133.
(9) Welsh, I. D.; Sherwood, P. M. A. *Proc. Electrochem. Soc.* **1989**, *89-13* (*Advances in Corrosion Protection by Organic Coatings*; Scantlebury, D., Kendig, M., Eds.), 417.
(10) Hutson, F. L.; Ramaker, D. E.; Koel, B. E.; Gebhard, S. C. *Surf. Sci.* **1991**, *248*, 119 and references therein.
(11) Hutson, F. L.; Ramaker, D. E.; Koel, B. E. *Surf. Sci.* **1991**, *248*, 104 and references therein.
(12) Carter III, R. O.; Gierczak, C. A.; Dickie, R. A. *Appl. Spectrosc.* **1986**, *40*, 649.
(13) Dickie, R. A.; Hammond, J. S.; Holubka, J. W. *Ind. Eng. Chem. Prod. Res. Dev.* **1981**, *20*, 339.
(14) Allara, D. L.; Nuzzo, R. G. *Langmuir* **1985**, *1*, 52.
(15) Boerio, F. J.; Chen, S. L. *J. Colloid Interface Sci.* **1980**, *73*, 176.
(16) Mino, N.; Tamura, H.; Ogawa, K. *Langmuir* **1991**, *7*, 2336.

0897-4756/93/2805-1554$04.00/0

exposure cell has been described elsewhere.[17,18] Both UHV systems could achieve a base pressure of 10^{-10} Torr. All XPS data were recorded in the fixed analyzer transmission (FAT) mode with a pass energy of 25 eV for core regions and 50 eV for valance-band regions. Unmonochromatized Mg Kα radiation (1253.6 eV) was used at a power of 275 W (12 kV, 25 mA). The spectrometer energy scale was calibrated using copper.[19] Peak positions were referenced to the C(1s) peak (284.6 eV) from surface hydrocarbon. Argon ion sputtering was carried out using a B21 saddle-field ion source sputter ion gun at 2.6 kV and 1 mA with an argon pressure of 10^{-3} Torr.

X-ray diffraction (XRD) studies were carried out with a Scintag XDS 2000 instrument. The X-ray radiation wavelength used was Cu Kα_1 (0.154 059 nm) with an X-ray power of 1800 W. The data were collected using the normal step-scanning mode with a step size of 0.02°. The samples were normally mounted in a Mylar tray.

The RAFTIR spectrum of the polymer film formed on the nickel surface was measured by using an FTIR spectrometer (BIO-RAD Digilab Division FTS-40 spectrometer) with a resolution of 4.0 cm^{-1}. The nickel substrate background was subtracted from the spectrum. For this measurement, a multiple internal reflection (MIR) technique was used. The angle of incidence was 45°. The details of the MIR technique are reported elsewhere.[16,20]

Sample Preparation. Etidronic acid was obtained from Monsanto. Calcium etidronate was obtained from International Paint. Sodium Chloride and nickel powder were obtained from Fisher. The NiO(green) used was from Strem, and the NiO-(black) was from Aldrich. Nickel etidronate was obtained as a precipitate formed after reaction of nickel powder or NiO(black) with etidronic acid for 3 days. Nickel phosphates were obtained by concentrating the solution resulting from the reaction of nickel powder with phosphoric acid for 1 week. Alfa nickel foil was used as the source of pure nickel (99.994% purity).

The nickel metal samples were polished mechanically with alumina (44 μm). No trace of aluminum was found on the polished metals on XPS examination. They were also degreased with acetone and cleaned with quadruple distilled water. The metals thus had only an air-formed film on the surface.

Two types of experiments were performed. The *ex situ* experiments were performed on the bench. The anaerobic experiments were performed in the special chamber discussed above. *Ex situ* experiments involved the exposure of the samples, cleaned as described above, to etidronic acid and calcium etidronate solution for eight hours in the atmosphere. Anaerobic experiments involved the further cleaning of the samples by argon ion sputtering for 1.5–2 h with surface purity monitored by XPS. The sample was rotated during the argon ion sputtering to allow even treatment of the sample. The clean sample was then exposed to a positive pressure of ultrahigh-purity (UHP) argon in the anaerobic cell and then dipped into dearated solutions of etidronic acid or calcium etidronate. The solutions were deaerated with UHP nitrogen for at least 8 h and then exposed to UHP argon for 10–15 min. The samples were then removed from solution and rinsed with daerated quadruply distilled water three times. Anaerobic cell experiments thus eliminate exposure of the sample to any oxygen in either the gaseous or solution state.

Etidronic acid (1 M), saturated calcium etidronate (~1 mM) and sodium chloride (1 M) solutions were prepared with quadruply distilled water.

Data Processing. Both smoothed and unsmoothed valance band XPS spectra are shown. The smoothed spectra were smoothed using a binomial smoothing method[21,22] with an interval of 13 and repeated 50 times. Nonlinear background removal was achieved using the Tougaard method.[23] O(1s) spectra were fitted using a nonlinear least-squares method with a Gaussian/Lorentzian peak shape,[24-26] including the effect of X-radiation satellites.

Table I. Conditions Used in Etidronic Acid Inhibitor Studies

case 1[a]	case 2[a]	case 3[b]	case 1[a]	case 2[a]	case 3[b]
1 h[c]			5 h[c]	5 h[c]	8 h[c]
3 h[c]			1 h[d]	1 h[d]	

[a] *Anaerobic cell* experiment. The sample was first argon ion etched and then exposed to the deoxygenated solution in the *anaerobic cell*. [b] *Ex situ* experiment. The sample with its air-formed oxide film was exposed to EDA solution in the atmosphere. [c] Exposure to deaerated 1 M EDA solution. [d] Exposure to deaerated 1 M NaCl solution.

Table II. XPS Peak Area Ratios[a]

solutions and exposure time[b]	C/O	C/P	C/Ni	O/P
1 h in EDA(A)	4.3	66.0	10.0	15.2
3 h in EDA(A)	4.4	30.1	22.0	6.8
5 h in EDA(A)	5.9	96.3	24.6	16.4
1 h in NaCl(A)	31.2	957.9	173.2	30.7
5 h in EDA(B)	10.5	171.2	87.5	16.3
1 h in NaCl(B)	8.4	P not seen	171.3	P not seen
8 h in EDA(C)	8.0	117.7	17.7	14.7
NiEDA	2.2	5.7	15.5	2.6

[a] The peak area ratios are adjusted for the atomic sensitivity factors from: *Practical Surface Analysis by Auger and Photoelectron Spectroscopy*; Briggs, D., Seah, M. P., Eds.; Wiley: London, 1990; Appendix 6, p 635. [b] (A) Case 1; (B) case 2; (C) case 3.

Results and Discussion

Nickel metal was exposed to etidronic acid for different exposure times and then exposed to sodium chloride solution for three different sample conditions as shown in Table I. No significant changes were found for exposure to calcium etidronate solution other than some nickel oxidation, so the results reported here are for 1 M solution of etidronic acid (EDA). The three cases compare the effect of several shorter exposures to EDA (case 1), compared to two longer exposures to EDA (cases 2 and 3).

Figure 1 shows the overall spectra that results from various experiments associated with the treatment methods described in Table I. Table II shows the atomic ratios of carbon, nickel, and phosphorus based upon the core XPS area ratios. These ratios indicate how the relative amount of carbon increases, and nickel and phosphorus decrease with increasing exposure time to EDA and exposure to sodium chloride solution. The ratios, however, assume that the sample probed is homogeneous (which is almost certainly not the case) and thus give only a crude guide to compound stoichiometry. For nickel etidronate the O/P ratio has a value (2.6) comparable to that expected for the etidronate ion (3.5), though the C/P ratio (5.7) is higher than expected for this ion (1.0) presumably because of the presence of surface hydrocarbon.

Core XPS Studies. The trends observed in the overall spectra are confirmed by a detailed examination of the Ni(2p), P(2p), and O(1s) core regions. The discussion below will focus on the results from the anaerobic cell, since in the *ex situ* experiments expose to EDA leads only

(17) Sherwood, P. M. A. *Chem. Soc. Rev.* **1985**, *14*, 1.
(18) Liang, Y.; Paul, D.; Xie, Y.; Sherwood, P. M. A. *Anal. Chem.* **1993**, *65*, 2276.
(19) *Surf. Interface Anal.* **1991**, *17*, 889 (ASTM, E902-88).
(20) Harrick, N. J. *Internal Reflection Spectroscopy*, 2nd ed.; Harrick Scientific Corp.: Ossining, New York, 1979.
(21) Marchand, P.; Marmet, L. *Rev. Sci. Instrum.* **1983**, *54*, 1034.
(22) Delamar, M. *J. Electron Spectrosc. Relat. Phenom.* **1990**, *53*, c1.
(23) Tougaard, S.; Sigmund, P. *Phys. Rev. B* **1982**, *25*, 4452.
(24) Ansell, R. O.; Dickinson, T.; Povey, A. F.; Sherwood, P. M. A. *J. Electrochem. Interfacial Electrochem.* **1979**, *98*, 79.
(25) Sherwood, P. M. A. In *Practical Surface Analysis by Auger and Photoelectron Spectroscopy*; Briggs, D., Seah, M. P., Eds.; Wiley: London, 1983; pp 445–475.
(26) Sherwood, P. M. A. In *Data Analysis in XPS and AES in Practical Electron Spectroscopy*; Briggs, D., Seah, M. P., Eds.; Wiley: New York, 1990; Appendix 3, pp 555–86.

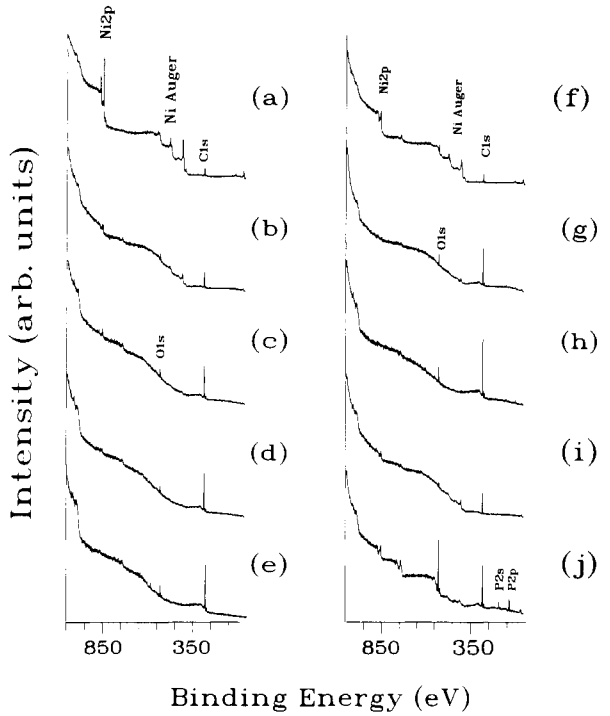

Figure 1. Overall XPS spectra of nickel metal exposed to etidronic acid (1 M) solution for different conditions, followed by exposure to sodium chloride (1 M) solution. The spectrum of nickel etidronate is provided for comparative purposes: (a) argon ion etched nickel metal; (b) sample (a) after exposure to EDA solution for 1 h in the anaerobic cell; (c) sample (b) after a further 2 h exposure to EDA solution giving a total of 3 h exposure; (d) sample (c) after a further 2 h exposure to EDA solution giving a total of 5 h exposure to EDA solution in the anaerobic cell; (e) sample (c) after exposure to sodium chloride solution for 1 h in the anaerobic cell; (f) argon ion etched nickel metal exposed to sodium chloride solution for 1 h in the anaerobic cell; (g) argon ion etched nickel metal exposed to EDA solution for 5 h in the anaerobic cell; (h) sample (g) after exposure to sodium chloride solution for 1 h in the anaerobic cell; (i) nickel metal with an air formed oxide film exposed to EDA solution for 8 h; (j) nickel etidronate.

to some nickel oxidation. Details of the core regions are given in Figures 2–4 and in Tables II and III.

The Ni(2p) spectra show that there is a more substantial reduction in Ni(2p) intensity when the etched metal is exposed to EDA for 1 h, then again for a further 2 h, again for a final 2 h, and these for one single 5-h exposure. In all cases the exposure of the film formed after EDA exposure to sodium chloride led to a thickening of the film as evidenced by the almost complete loss of Ni(2p) intensity. When the *ex situ* sample is exposed to EDA for 8 h, the Ni(2p) spectrum is characteristic of oxidized nickel, indicating that the formation of the carbon-containing film is dependent upon an initially clean and unoxidized nickel metal surface.

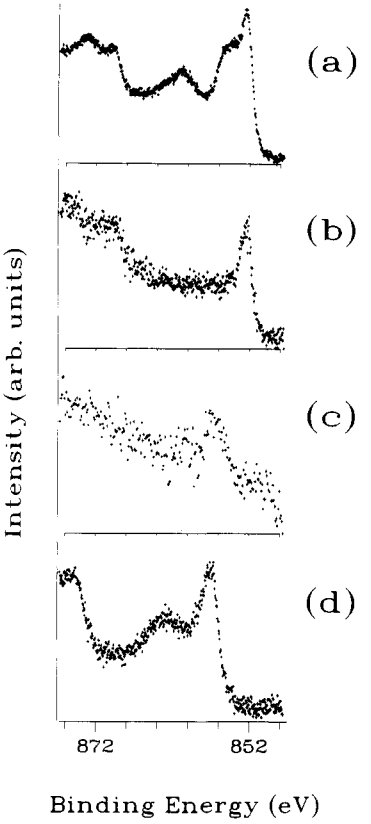

Figure 2. Ni(2p) core XPS spectra of nickel metal exposed to etidronic acid (1 M) solution for different conditions, followed by exposure to sodium chloride (1 M) solution. The spectrum of nickel etidronate is provided for comparative purposes: (a) argon ion etched nickel metal exposed to sodium chloride solution for 1 h in the anaeroobic cell, (b) argon ion etched nickel metal exposed to EDA solution for 5 h in the anaerobic cell; (c) sample (b) exposed to sodium chloride solution for 1 h in the anaerobic cell; (d) nickel etidronate.

Figure 2 illustrates how sodium chloride solution causes oxidation of the clean metal (Figure 2a). However, exposure to EDA still shows a largely unoxidized metal with a thick carbon-containing overlayer (Figure 2b). Exposure of the EDA-treated sample to sodium chloride solution leads to a thickening of the film as evidenced by the almost complete loss of Ni(2p) intensity giving a very weak nickel feature that may correspond to some nickel etidronate at the interface of the metal and outer film (Figure 2c,d).

Very little phosphorus is present in the film as shown in Figure 3 and Table II, allowing one to discount the possibility that the changes are caused by adsorption of EDA onto the nickel surface. It is reasonable to suppose that phosphorus is lost from the film as a water soluble phosphate resulting from EDA decomposition, and that there was hardly any nickel etidronate formation. It is

Table III. XPS Results for O(1s)/Ni Auger Regions

solutions and exposure time[a]	peak 2 (531.5) fwhm = 1.9, %	peak 3 (532.0) fwhm = 1.9, %	peak 4 (532.9) fwhm = 1.9, %	peak 5 (533.5) fwhm = 1.9, %
h in EDA (A) (Figure 4b)	63.4		27.8	
3 h in EDA (A) (Figure 4c)	55.5		39.3	
5 h in EDA (A) (Figure 4d)	44.2		47.8	
1 h in NACl (A) (Figure 4e)	15.3		82.1	
5 h in EDA (B) (Figure 4g)	10.6		84.1	
1 h in NaCl (B) (Figure 4h)	3.8		88.4	
8 h in EDA (C) (Figure 4i)	59.0		23.4	6.8
NiEDA (Figure 4j)		54.8		38.4

[a] (A) Case 1; (B) case 2; (C) case 3.

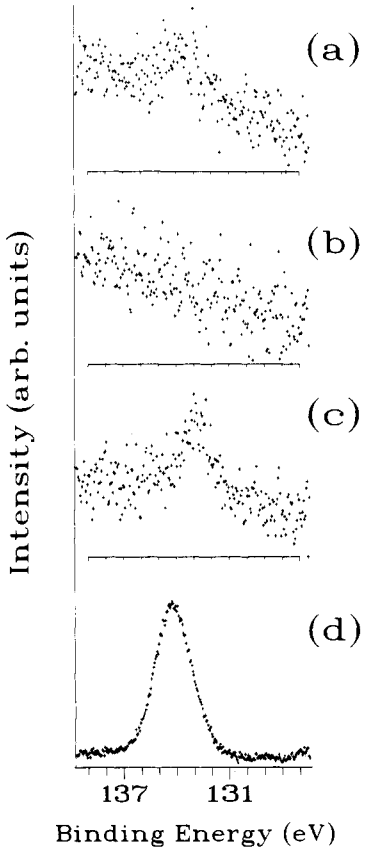

Figure 3. P(2p) core XPS spectra of nickel metal exposed to etidronic acid (1 M) solution for different conditions, followed by exposure to sodium chloride (1 M) solution. The spectrum of nickel etidronate is provided for comparative purposes: (a) argon ion etched nickel metal exposed to EDA solution for 5 h in the anaerobic cell; (b) sample (a) exposed to sodium chloride solution for 1 h in the anaerobic cell; (c) nickel metal with an air formed oxide film exposed to EDA solution for 8 h; (d) nickel etidronate.

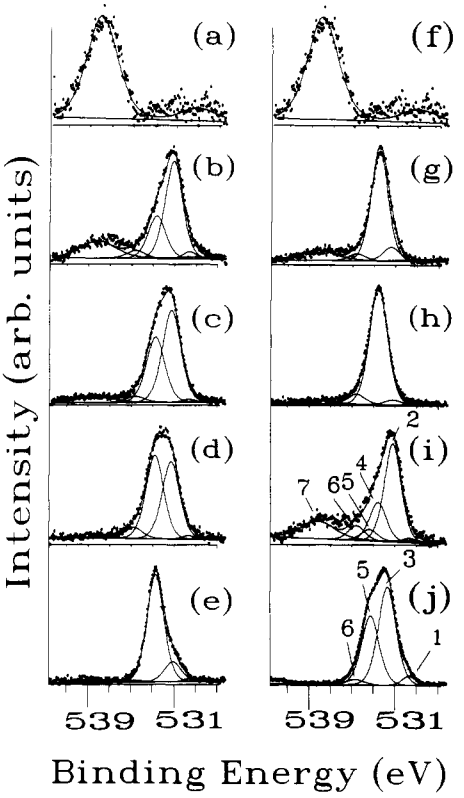

Figure 4. O(1s) core XPS spectra of nickel metal exposed to etidronic acid (1 M) solution for different conditions, followed by exposure to sodium chloride (1 M) solution. The spectrum of nickel etidronate is provided for comparative purposes: (a) argon ion etched nickel metal; (b) sample (a) after exposure to EDA solution for 1 h in the anaerobic cell; (c) sample (b) after a further 2h exposure to EDA solution giving a total of 3 h exposure; (d) sample (c) after a further 2 h exposure to EDA solution giving a total of 5 h exposure to EDA solution in the anaerobic cell; (e) sample (c) after exposure to sodium chloride solution for 1 h in the anaerobic cell; (f) argon ion etched nickel metal; (g) argon ion etched nickel metal exposed to EDA solution for 5 h in the anaerobic cell; (h) sample (g) after exposure to sodium chloride solution for 1 h; (i) nickel metal with an air formed oxide film exposed to EDA solution for 8 h; (j) nickel etidronate.

not possible to distinguish between etidronate and phosphate since their P(2p) core binding energies are almost identical; however, they can be distinguished in the valence band region (see below). The large values for the O/P atomic ratio indicates that P/O species will make little contribution to the O(1s) region (except in the case of NiEDA).

The O(1s) region, which also includes the Ni $L_2M_{23}M_{23}$ Auger region, is illustrated in Figure 4 with fitting details given in Table III. Figure 4i identifies the positions of peaks 2, 4, 5, 6, 7, and Figure 4j the positions of peaks 1, 3, 5, and 6. Table III shows only the major components (peaks 2–5) in the spectrum. Peak 1 never represents more than 4% of the spectrum, and peak 6 no more than 9% of the spectrum. The spectra can be fitted without these peaks, but their inclusion does improve the quality of the fit. The region confirms how the Ni Auger feature at 538.6 eV diminishes in intensity with respect to the O(1s) features at higher binding energy as the etched metal is exposed to EDA in the anaerobic cell. The O(1s) region can be fitted to several features consistent with NiO at 529.9 eV[18,27] (peak 1) with a width of 1.4 eV corresponding to the previously observed width for this peak;[18] $Ni(OH)_2$, water, singly bonded P/O features, and multiply bonded oxygen features involving carbon (such as C=O) around 531.5 eV (peak 2), and single bonded oxygen features mainly involving carbon (such as C–OH, C–O–C), and doubly bonded P/O[27–30] at 532.9 eV (peak 4) that may also include features due to adsorbed water. Nickel etidronate had a peak at 532.0 eV (peak 3) and another peak at 533.5 eV (peak 5) which may correspond to single and doubly bonded P/O features respectively.[30–32] Peak 6 may also be due to adsorbed water, but its small contribution in most spectra makes its presence uncertain.

The curve-fitting results show that carbon–oxygen multiple bond functionality around 531–532 eV (peak 2) is the dominant feature for the samples treated in the *anaerobic cell.* Features in the range 533 eV (peak 4) corresponding to carbon–oxygen single-bond functionality increase as the exposure time to EDA increases in Figure

(27) Fontaine, R.; Feve, L.; Buvat, J. P.; Schoeller, C.; Caillat, R. *J. Micro. Spectrosc. Electron* **1989**, *14*, 453.

(28) López, G. P.; Castner, D. G.; Ratner, B. D. *Surface Interface Anal.* **1991**, *17*, 267.

(29) Kozlowski, C.; Sherwood, P. M. A. *Carbon* **1987**, *25*, 751.

(30) Schuetzle, D.; Carter III, P. O.; Shyu, J.; Dickie, R. A.; Holubka, J.; McIntyne, N. S. *Appl. Spectrosc.* **1986**, *40*, 641.

(31) Rizkalla, C. N. *Inorg. Chim. Acta* **1982**, *60*, 53.

(32) Koudelka, M.; Sanchez, J.; Augustyński, J. *J. Electrochem. Soc.* **1982**, *129*, 1186.

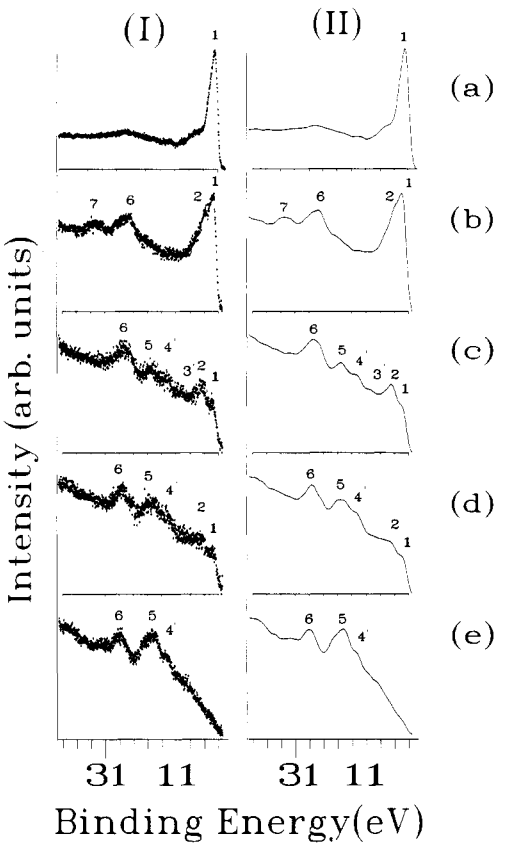

Figure 5. Valence band XPS spectra of nickel metal exposed to etidronic acid (1 M) solution for different conditions, followed by exposure to sodium chloride (1 M) solution. The spectrum of nickel etidronate is provided for comparative purposes. The original spectra are shonw in (I), and spectra smoothed by a binomial smoothing process are shown in (II): (a) argon ion etched nickel metal; (b) argon ion etched nickel metal exposed to EDA solution for 5 h in the anaerobic cell; (c) sample (b) exposed to sodium chloride solution for 1 h in the anaerobic cell; (d) nickel metal with an air formed oxide film exposed to EDA solution for 8 h; (e) nickel etidronate formed by reaction of nickel powder with EDA for 3 days; (f) nickel etidronate formed by reaction of NiO (black) powder with EDA for 3 days.

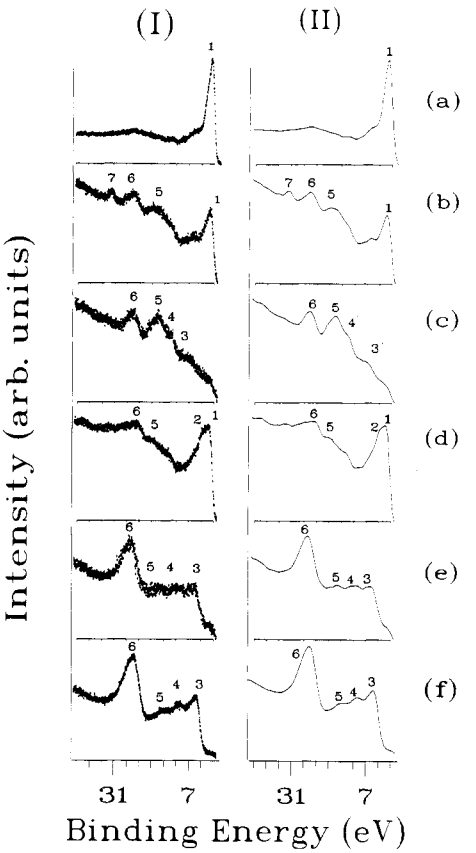

Figure 6. Valence band XPS spectra of nickel metal exposed to etidronic acid (1 M) followed by exposure to sodium chloride (1 M) solution in the anaerobic cell. The conditions used correspond to case 1 in Table I: (a) argon ion etched nickel metal; (b) sample (a) after exposure to EDA solution for 1 h; (c) sample (b) after a further 2 h exposure to EDA solution giving a total of 3 h exposure; (d) sample (c) after a further 2 h exposure to EDA solution giving a total of 5 h exposure to EDA solution; (e) sample (c) after exposure to sodium chloride solution for 1 h.

4 (b–d). There is a marked increase in the amount of carbon–oxygen single-bonded species on exposure to sodium chloride solution (Figure 4e), and in the 5-h continuous exposure experiment (Figure 4g). Features due to phosphate and/or EDA would also occur in the region of peak 4, but the high O/P ratio especially after sodium chloride treatment means that they would make a very small contribution to this region. Exposure to EDA in the *ex situ* experiment leads to the formation of a nickel hydroxide peak at around 531.5 eV—typical of a metal hydroxide O(1s) feature. The implications of these observations are that the initial hydrocarbon species is largely C/O double bonded but becomes single bonded as the film thickens, and especially after exposure to sodium chloride solution. The thickness and stability of the film are consistent with the formation of a polymeric film, and we will see below that this is confirmed by the RAFTIR results.

The C(1s) spectrum is similar for most experiments but does broaden and shows asymmetry to higher binding energy after sodium chloride treatment following case 1 (Table I) treatment.

Valence Band Spectra. Figures 5 and 6 show the corresponding valence band regions. Figure 5 shows samples exposed to cases 2 and 3 (table I) together with spectra corresponding to two different preparations of nickel etidronate. Figure 6 shows samples exposed to case 1 (Table I) conditions. Figure 4b–e shows the O(1s)/Ni Auger regions corresponding to Figure 6b–e and Figure 4g–j the same regions corresponding to Figure 5b–e. These spectra show how the nickel etidronate spectra (Figure 5 e,f) are very different from those of the other valence band spectra. In fact the nickel etidronate spectra show a spectrum typical of the etidronate ion reported in our earlier work.[8,9] This provides a good illustration of how the valence band region can be especially helpful in distinguishing species that cannot necessarily be unambiguously distinguished in the core region. XRD studies (discussed below) show that the nickel etidronate sample does not correspond to nickel phosphate, consistent with our previous experimental and theoretical studies that show that the valence band region can clearly distinguish between phosphate and etidronate.

It is interesting to note that we can prepare nickel etidronate by reaction of EDA with nickel powder or black nickel oxide. The nickel powder result is not surprising since, as with most powder samples, this powder has a high surface area and thus a significant area of exposed surface oxide. We were unable, however, to get any reaction between green nickel oxide and EDA. We attribute this differece between green and black nickel

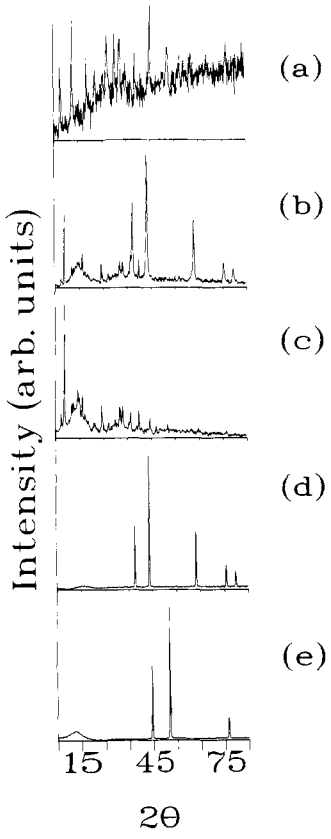

Figure 7. X-ray diffraction patterns of various nickel compounds: (a) nickel phosphate; (b) nickel etidronate produced by reaction of NiO with EDA for 3 days; (c) nickel etidronate produced by reaction of nickel powder with EDA for 3 days; (d) NiO (black); (e) nickel powder.

oxide to the presence of Ni(III) ions in the latter compound. Presumably some Ni(III) is needed to initiate reaction between EDA and the oxide.

The contrast between the anaerobic cell results and those of the *ex situ* experiment is clearly shown in Figures 5 and 6. Thus feature 6, a principally O(2s) feature, is present in all the spectra. However the etidronate spectral feratures 3, 4, and 5 are distinctive, as are the nickel metal (1) and oxide (2) features. Feature 5 is a typical hydrocarbon feature corresponding to a principally C(2s) region. The *ex situ* experiment gives a largely oxidized nickel metal spectrum, with some hydrocarbon (Figure 5d). The anaerobic cell nickel metal exposure experiments clearly show a high level of oxidized hydrocarbon, with a hydrocarbon content that is substantially increased on exposure to sodium chloride solution. It is important to note that no residual sodium chloride is present on the surface as evidenced by the absence of a Na(3s) feature around 32 eV in the valence band spectra. Feature 7 is only seen in the case of the 1 h (Figure 5b) and 5 h continuous (Figure 6b) EDA exposure experiments. We believe that this feature (probably a satellite) corresponds to Ni(III) possibly resulting from some initial oxidation of the nickel by the EDA exposure. It may be that this leads to some nickel etidronate formation, since the presence of Ni(III) seems to be a requirement for this process, and then the nickel etidronate decomposes leading to polymer formation. Features 4′ and 3′ are largely O(2p) and C(2p) features associated with the hydrocarbon polymer film. The valence band spectrum of the nickel metal exposed to EDA in the anaerobic cell is consistent with an oxidized

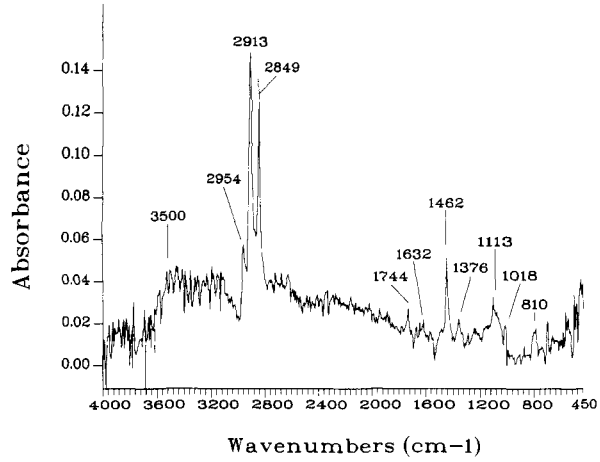

Figure 8. Reflection absorption Fourier transform infrared (RAFTIR) spectrum of the polymer film formed on the clean nickel metal surface by reaction with EDA in the anaerobic cell.

hydrocarbon polymer spectrum,[33] and this combined with our RAFTIR results leads us to suggest that a polymer is formed.

Figure 6 shows the changes in the valence band spectrum wtih the exposure time to EDA in the anaerobic cell. After the first 1-h exposure, the signal of oxidized nickel was obvious. With the increasing exposure time, the spectral features due to oxidized hydrocarbon polymer became more and more significant, and the Ni(3d) signals, from both nickel metal and oxidized nickel, decrease substantially. After exposure to sodium chloride solution, the Ni(3d) signal totally disappeared. The greater thickness of the polymer film for case 1 of Table I compared to case 2 of Table I is confirmed by the valence band spectra.

One might suggest that the carbon was caused by contamination. However, C(2s) is generally of much lower intensity than the metal valence band features, and after very many valence band studies in our laboratory it is clear that this level of carbon is not seen even on the most contaminated samples. It is also significant to note that the high levels of carbon are found only in the anaerobic cell experiments and not the *ex situ* experiments. Since the latter experiment would be expected to lead to more surface hydrocarbon contamination, this further eliminates contamination as the source of carbon. Finally the ability to record an oxidized hydrocarbon spectrum by FTIR clearly shows that this a film of considerable thickness.

XRD Studies. Figure 7 shows the X-ray powder diffraction patterns for various nickel compounds confirming the similarity in pattern for the two nickel etidronate samples (from nickel powder and black nickel oxide) shown in Figure 7b,c. The substantial difference between the pattern for the etidronate samples and nickel phosphate is clear. It is also clear that the nickel etidronate sample prepared from the black nickel oxide has an underlying layer of nickel oxide. This underlying layer is not seen in the valence band XPS data since the XRD studies give bulk rather than surface information.

RAFTIR Studies. The film formed on the nickel surface after five hours exposure to EDA in the anaerobic cell experiment was sufficiently thick to be visible. It was examined by RAFTIR giving the spectrum shown in Figure 8. The spectrum is in good agreement with that of an

(33) Xie, Y.; Sherwood, P. M. A. *Appl. Spectrosc.* **1991**, *45*, 1158 and references therein.

Table IV. Infrared Spectrum and Mode Assignments for the Film Formed on the Clean Nickel Surface Exposed to Etidronic Acid in the *Anaerobic Cell*

frequency, cm^{-1}	mode[a]	ref
3500 (br)	ν OH	15
2954	ν C–H, CH_3, asym str	13, 14
2913	ν C–H, CH_2, asym str	14, 15
2849	ν C–H, CH_2, sym str	14, 15
1744	C=O str	14
1632	C=C str	14, 34
1462	$-CH_2$, scissors def, aliphatic ether carbon	14, 13
1376	C–C(CH_3) methyl def	13
1220	ν C–O ether asym; ν P=O and P–O–H out-of-plane def	13
1113	ν C–C; ν C–C(CH_3)$_2$ skeletal; C–O–H def secondary alcohol	13
1018	C–O–H def primary alcohol	13
810	C–C(CH_3)$_2$ skeletal def	13

[a] The following symbols are used: str, stretching; asym, asymmetric; sym, symmetric; br, broad; def, deformation.

oxidized hydrocarbon polymer, and the assignments are given in Table IV. In agreement with the XPS data it can be seen that both single and doubly bonded C/O functionality is found.

It is obvious that the film was composed of hydrocarbon. The most intense peaks were at 2913 and 2849 cm^{-1}, which belong to asymmetric and symmetric C–H stretching vibration modes of the CH_2 group. The peak at 1462 cm^{-1} was caused by the scissors deformation mode of CH_2 or the vibration mode of aliphatic carbon. All of the intense peaks were caused by the $-CH_2$ group. The peaks caused by $-CH_3$ groups were of very low intensity. This suggests that there were very few $-CH_3$ terminal groups in this film, indicating that the film was mainly composed of long-chain aliphatic hydrocarbon bonds. Single-bonded oxygen corresponded to both hydroxyl groups and ether groups.

Role of Chloride Ions. Sodium chloride solution appears to thicken the protective film as can be seen by comparison of the Ni(2p) spectra (Figure 2b vs 2c) and the valence band spectra (Figures 5b,c and 6d,e). One needs to consider how it is possible for the film to become thicker even though nothing other than sodium chloride solution was added to the sample. One notes in Table II that there is a 10-fold or greater increase in the C/P atomic ratio after addition of sodium chloride solution, indicating that addition of this solution causes loss of phosphorus from the sample, presumably as soluble phosphate. This result would thus be consistent with additional hydrocarbon polymer being formed by chloride ions enhancing the decomposition of EDA, already present in the samples after their 5-h exposure to EDA, to give more hydrocarbon polymer. Support for such a supposition is provided by the work of Growcock and co-workers of steel corrosion inhibition in hydrochloric acid inhibited with *trans*-cinnamaldehyde.[35-38] These workers discussed the inhibition mechanism,[35] showed that chloride ions enhanced the adsorption of the *trans*-cinnamaldehyde onto the steel surface, and found that the cinnamaldehyde polymerized on the surface.[35,37] They suggested, on the basis of kinetic studies, that the bound *trans*-cinnamaldehyde then polymerizes in a process involving chloride ions. The polymer was found to be complex mixture of low molecular weight aromatic hydrocarbon polymers, including polyenes.[37]

Conclusions

It is clear that a polymeric film of considerable thickness is formed on a nickel surface after exposure of the clean metal in an anaerobic environment to etidronic acid solution. The resulting film consists of both singly and double bonded C/O functionality but contains no phosphorus and nickel. The film is sufficiently thick as to obscure the underlying nickel metal in XPS studies and to be examined by FTIR. It would appear that the film has protective powers, showing no nickel oxidation when the metal covered with the film is exposed to the aggressive sodium choride solution. The behavior of the more corrosion resistant nickel metal to etidronic acid is in contrast to the more active metal iron. In the case of iron an etidronate film is formed on the metal surface that can react with the native oxide film to form phosphate.[8] In both the cases of iron and nickel some corrosion protection is provided by etidronic acid but by a completely different mechanism. It seems that the formation of the polymeric film in nickel may be an effective corrosion protection; however, it is possible to form such a film only if the metal has no surface oxidation. Thus while the results reported here may not have immediate practical application for corrosion inhibition for air-oxidized nickel, the observation of this type of protective film shows the potential for the development of corrosion protective agents that can chemically react with a metal surface to form protective polymer films. Recent studies have reported the presence of polymeric films on the surface of iron and steel exposed to zinc dithiophosphate,[39] nickel exposed to (2-pentylamino)benzimidazole,[40,41] and steel exposed to *trans*-cinnamaldehyde.[35-38] This work thus provides further support for the utility of such polymeric films in corrosion inhibition.

Acknowledgment. This material is based upon work supported by the National Science Foundation under Grant No. CHE-8922538. We are grateful to the U.S. Department of Defense for funding the X-ray diffraction equipment.

(34) Bellamy, I. J. *The Infrared spectra of Complex Molecules*; Wiley; New York, 1975 and references therein.

(35) Growcock, F. B.; Frenier, W. W. *J. Electrochem. Soc.* **1988**, *135*, 817.

(36) Growcock, F. B.; Lopp, V. R.; Jasinski, R. J. *J. Electrochem. Soc.* **1988**, *135*, 823.

(37) Growcock, F. B.; Lopp, V. R. *Corrosion* **1988**, *44*, 248.

(38) Growcock, F. B. *Corrosion* **1989**, *45*, 1003.

(39) Ludwig, S.; Wagner, K.; Braatz, G. *Schmierungstechnik* **1983**, *14*, 312.

(40) Goledzinowski, M. M.; Haupt, S.; Schultze, J. W. *Electrochim. Acta* **1984**, *29*, 493.

(41) Goledzinowski, M. M.; Rolle, D.; Schultze, J. W. *Werkst. Korros.* **1985**, *36*, 381.